(29) Benedetti, E.; Pedone, C.; Allegra, G. *Macromolecules* **1970**, *3*, 16–19.
(30) The actual computational effort is much less than the number of iterative steps multiplied by the effort for the first minimization, since the final estimate of the Hessian matrix found in the minimization in one step is used as an initial estimate for the Hessian in the next step (the estimation of this matrix being the most laborious part in the minimization), and this estimate becomes rapidly better as the iterative scheme proceeds, making the minimizations in the iterative scheme successively more and more efficient.
(31) Flory, P. J. "Principles of Polymer Chemistry", 10th ed.; Cornell University Press: Ithaca, NY, 1978; p 254.
(32) Richardson, J. W.; Parks, G. S. *J. Am. Chem. Soc.* **1939**, *61*, 3543–3546.
(33) Evans, A. G.; Polanyi, M. *Nature (London)* **1943**, *152*, 738.
(34) Parks, G. S.; Mosher, H. P. *J. Polym. Sci., Polym. Chem. Ed.* **1963**, *1*, 1979–1984.
(35) Biddlup, R. H.; Plesch, P. H.; Rutherford, P. P. *Polymer* **1960**, *1*, 521.
(36) Miyazawa, T. *J. Polym. Sci.* **1961**, *55*, 215–231.
(37) In our notation, Miyazawa's formulas are

$$\cos(\alpha/2) = \cos\left(\frac{\varphi_i + \varphi_{i+1}}{2}\right)\cos(\theta'/2)\cos(\theta''/2) + \cos\left(\frac{\varphi_i - \varphi_{i+1}}{2}\right)\sin(\theta'/2)\sin(\theta''/2)$$

and

$$d = 2l\sin\left(\frac{\varphi_i + \varphi_{i+1}}{2}\right)\cos(\theta'/2)\cos(\theta''/2)/\sin(\alpha/2)$$

(38) Abramowitz, M.; Stegun, I. A. "Handbook of Mathematical Functions"; *Natl. Bur. Stand. (U.S.) Circ.*, p 884.
(39) Suter, U. W.; Flory, P. J. *Macromolecules* **1975**, *8*, 765–776.
(40) p 73 ff of ref 25.
(41) Flory, P. J. *Macromolecules* **1974**, *7*, 381–392.
(42) Flory, P. J.; Mandelkern, L.; Kinsinger, J. B.; Shultz, W. B. *J. Am. Chem. Soc.* **1952**, *74*, 3365–3367.

Configuration of the Polyisobutylene Chain according to Neutron and X-ray Scattering

Hisao Hayashi† and Paul J. Flory*

IBM Research Laboratory, San Jose, California 95193

George D. Wignall

National Center for Small-Angle Scattering Research, Oak Ridge National Laboratory, Oak Ridge, Tennessee 37830. *Received January 17, 1983*

ABSTRACT: The dimensions and configurations of polyisobutylene (PIB) chains in the bulk and in solution have been investigated by neutron and X-ray scattering at small and at intermediate angles. Measurements in bulk were carried out by neutron scattering on protonated PIB (PIB-H) dispersed in matrices consisting either of fully deuterated PIB-d_8 or of the hexadeuterio polymer, PIB-d_6, in which only the methyl groups are deuterated. Neutron scattering from PIB-H dissolved in benzene-d_6 at 26.4 °C provided results in a Θ-solvent, and X-ray scattering measured in *n*-heptane allowed observations on the configurations as represented by carbon scattering centers. The *z*-average radii of gyration, $\langle s^2\rangle_z^{1/2}$, were calculated from Zimm plots in the Guinier region. Values of $\langle s^2\rangle_z^{1/2}$ measured in the bulk (75 ± 5 Å) and in the Θ-solvent (77 ± 5 Å) are in good agreement. Results of scattering measurements at intermediate angles were compared by use of Kratky plots on an absolute scale, i.e., $F_x(\mu) = (x+1)\mu^2P(\mu)$ vs. μ, where μ is the magnitude of the scattering vector, $x+1$ the number of monomer units per chain, and $P(\mu)$ the normalized scattering function. The scattering curves for PIB-H observed in the PIB-d_8 matrix and in the Θ-solvent are in excellent accord in the range of $0 < \mu < 0.6$ Å^{-1}. These results demonstrate that the configuration in the bulk is virtually the same as in a Θ-solvent. The experimental data were compared also with theoretical scattering functions calculated on the basis of the conformational analysis of random PIB chains presented in the preceding paper. Five absolute Kratky functions $F_x(\mu)$ were calculated for scattering points consisting of (i) all eight protons, (ii) six methyl protons, (iii) two methylene protons, (iv) all four carbon atoms, and (v) only the substituted carbons in the monomer unit. These five functions differ appreciably for larger values of μ, indicating the importance of a proper choice of scattering points when calculations are compared with experimental curves. The first function (i) was compared with the experimental neutron scattering curves for PIB-H in the PIB-d_8 matrix and in the Θ-solvent, the second (ii) with that observed in the PIB-d_6 matrix, and the fourth (iv) with the X-ray scattering curve observed in solution. Close agreement throughout the range of μ covered by the experiments confirms the conformational analysis of PIB and demonstrates randomness of configurations in the bulk down to distances of ca. 10 Å.

Introduction

Recent applications of neutron scattering to studies of polymers[1] have provided much valuable information inaccessible by other methods. In particular, elastic scattering experiments with isotopically labeled polymers have succeeded in characterizing chain configurations in condensed systems such as bulk polymers and concentrated solutions. These experiments take advantage of the characteristics of hydrogen and deuterium whereby they differ in scattering length for neutrons while conferring closely similar thermodynamic properties on the polymer. A protonated polymer dispersed in a deuterated matrix (or vice versa) yields particle scattering that is unaffected by intermolecular interference and hence provides information on its intramolecular configurations. This method, applied to small-angle scattering by various polymers,[2-9]

† On leave from the Department of Polymer Chemistry, Kyoto University, Kyoto 606, Japan.

0024-9297/83/2216-1328$01.50/0

has demonstrated that chain dimensions in the amorphous bulk state and in the melt are the same as those in Θ-solvents, thus providing compelling evidence for the theoretical prediction[10] that the chain configurations in amorphous and liquid polymers are substantially unperturbed. Since the average chain dimensions have been confirmed to be unperturbed, it is reasonable to postulate that the local configurations are also unbiased; otherwise the configuration of the chain as a whole should be perturbed due to the accumulated effects of perturbations in local configurations. One may nevertheless contend, although the possibility seems remote, that the effects of local perturbations could somehow be compensated by alteration of the configuration of the chain as a whole in such a manner as to yield unperturbed overall dimensions.

In order to address this issue, measurements on the local configurations in the bulk and in a Θ-solvent need to be carried out. Intermediate-angle scattering has been proven to be suitable for this purpose because of its dependence on, and sensitivity to, correlation distances corresponding to those between scattering elements separated by comparatively short bond sequences within a polymer chain.[2,5,11,12]

In this study, we have measured elastic neutron scattering by labeled polyisobutylene (PIB) at intermediate angles as well as at small angles, and compared the results of scattering measurements observed in the bulk and in dilute solutions in a Θ-solvent. Experiments in the bulk were performed on protonated PIB (PIB-H) dispersed in matrices consisting either of fully deuterated PIB (PIB-d_8) or of hexadeuterio-PIB (PIB-d_6) in which only methyl protons were deuterated. In the former experiment, scattering by all protons in PIB-H molecules is observed, while in the latter matrix scattering is confined to methyl protons in the same molecules. Combination of these experiments, therefore, enables us to observe two different scattering functions for the same underlying configuration. Neutron scattering experiments in a Θ-solvent were carried out on PIB-H dissolved in deuteriobenzene (benzene-d_6). The absence of hydrogen atoms in this solvent maximizes the contrast between solute and solvent and minimizes incoherent scattering from protons. X-ray scattering at intermediate angles was also measured on PIB-H in solution. The carbon atoms that are the principal scattering elements for X-rays occupy locations displaced appreciably from the protons that are the points of contrast in the neutron scattering experiments.

Experimental scattering curves have been compared with the theoretical scattering functions computed by a Monte Carlo method on the basis of torsional angles for an appropriate set of rotational isomeric states and their statistical weights determined from the conformational analysis of PIB reported in the preceding paper,[13] hereafter referred to as I. Individual atoms were treated as scattering elements. The validity of the configurational–statistical treatment[13] of PIB is thus subjected to rigorous examination.

Experimental Section

(1) Sample Preparation. (a) Materials. Protonated PIB (PIB-H) was refined by fractional precipitation of a commercially available polyisobutylene (Vistanex LM-MS; Enjay Chemical Co.) from a 1% solution in benzene at 28 °C with methanol as precipitant. After fractions of high and low molecular weights had been discarded, the solution containing the middle portion, comprising ca. 40% of the original polymer, was evaporated to dryness at 100 °C under vacuum. The deuterated polymers, PIB-d_8 and PIB-d_6, were prepared by Prof. Kennedy of the University of Akron by cationic polymerization of the corresponding deuterated monomers using $EtAlCl_2$ as catalyst in dichloromethane at −75 °C. The degrees of deuteration of the monomers were greater than 99% of the formular values according to the supplier (Merck and Co.). These deuterated polymers served as matrices without fractionation. The molecular weights of these polymers are listed in Table I; the weight-to-number-average ratio for PIB-H also is included. The isotopic purity of benzene-d_6 and cyclohexane-d_{12} used as solvents for neutron scattering measurements was 99.5%.

Table I
Molecular Weights of Polymer Samples

polymer	M_w	M_v	M_w/M_n
PIB-H	46 000[a]	42 000[b]	1.3,[a]
PIB-d_8	60 000[c]		
PIB-d_6	300 000[c]		

[a] Measured in tetrahydrofuran (THF) by GPC equipped with a light scattering photometer. [b] Measured in toluene at 30 °C. [c] Measured by GPC in THF.

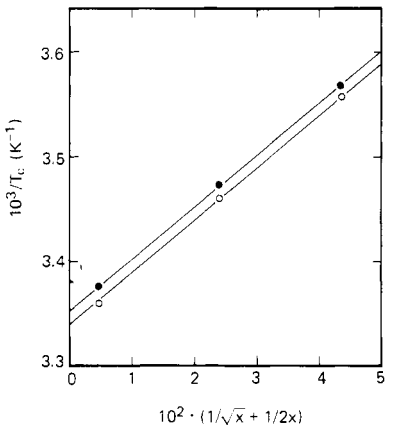

Figure 1. Shultz–Flory plots for determination of Θ-temperatures for protonated PIB-H in benzene-d_6 (○) and in hydrogenous benzene (●), yielding Θ = 26.4 ± 0.5 and 25.0 ± 0.5 °C, respectively.

(b) Scattering Samples. Weighed amounts of host and guest polymers were dissolved in cyclohexane at a combined concentration of ca. 1%, solvent was removed by evaporation, and the residue was dried at 100 °C under vacuum. The mixture of protonated PIB in the deuterated host polymer was pressed between a pair of quartz disks 1.6 mm thick, with a spacer of an appropriate thickness between them, and held at 100 °C under vacuum until all bubbles were removed. The samples of pure PIB-H and pure PIB-d_8 were prepared similarly. Samples containing or consisting of PIB-d_6 were hot pressed at 150 °C after mixing, a spacer slightly thicker than the desired sample thickness being used; in other respects the procedure was the same as described above. These modifications were required because of the higher molecular weight of PIB-d_6 and its resulting higher viscosity. Thicknesses of the samples were varied from 0.5 to 3 mm, depending on their scattering powers. Scattering measurements were carried out at room temperature, 21 ± 1 °C.

The solutions used for neutron scattering experiments were contained in a quartz cell 5 mm in length with windows 1.25 mm in thickness. They were kept at 26.4 ± 0.1 °C, the Θ-temperature (see below), by circulating thermostated water during the measurements. Samples for X-ray scattering were contained in an aluminum cell 4 mm in length with a pair of mica windows ca. 10 μm thick. Measurements were carried out at 25.0 ± 0.1 °C.

(2) Θ-Temperature. The Θ-temperature of PIB-H in benzene-d_6 was determined from measurements of critical consolute temperatures T_c by plotting $1/T_c$ against $1/x^{1/2} + 1/2x$, where x is the ratio of molar volumes of the polymer and the solvent.[14] From the plot shown in Figure 1, the Θ-temperature for this system was determined to be 26.4 ± 0.5 °C. The Θ-temperature for PIB-H in hydrogenous benzene was also measured for reference. A value of 25.0 ± 0.5 °C was obtained, in good agreement with previous results.[15]

(3) Neutron Scattering. (a) Apparatus. Neutron scattering was measured at the 30-m SANS facility of the National Center

for Small-Angle Scattering Research at the Oak Ridge National Laboratory. The neutron beam produced by the high-flux isotope reactor is monochromated by six pairs of pyrolytic graphite crystals and filtered with either cold beryllium or graphite to yield first- and second-order diffracted wavelengths λ of 4.75 and 2.38 Å, respectively. The monochromaticity $\Delta\lambda/\lambda$ is ±6% at both wavelengths, which is small enough for the present purpose.[16] A monitor counter is placed after the filter to detect the decay and fluctuation of the incident beam intensity. The monochromated neutron beam was collimated with a pair of pinholes serving as monochromator and sample slits located 7.5 m apart. A monochromator slit of 2.5-cm diameter was used for measurements at small angles and 3.5-cm diameter for intermediate angles. The diameter of the sample slit was 0.75 cm for bulk samples and 1.4 cm for solutions. Scattered intensity was measured with a two-dimensional position-sensitive detector, the active area of which is 64 × 64 cm^2, with detector elements of 1 × 1 cm^2. The sample-to-detector distance was varied from 1.3 to 12 m according to the angular range of measurement.

(b) Data Analysis. The two-dimensional scattering data were first normalized to 1000 counts of the monitor counter in order to correct for the variation of the incident beam intensity (<2% over a period of 24 h). The background due to electronic noise, cosmic rays, stray radiation, and scattering from the sample cell was subtracted. The normalized and background-corrected data were corrected for the inhomogeneity of the detector sensitivity at different detector elements by dividing the scattering from the sample by the isotropic scattering of water. The circular average was calculated for the two-dimensional data to obtain the one-dimensional scattering curve, i.e., the corrected and normalized scattered intensity vs. the magnitude of the scattering vector defined by $\mu = (4\pi/\lambda)\sin\theta$, where λ is the wavelength and θ is half of the scattering angle. Detailed descriptions of the camera, detector, and data acquisition system have been published elsewhere.[17,18]

(c) Incoherent Scattering. The coherent scattering from PIB-H dispersed in the matrix or dissolved in the solvent was obtained after subtracting both the incoherent background due to protons and the coherent scattering from the matrix or the solvent. The incoherent scattering due to the protons in PIB-H and PIB-d_6 was subtracted by comparison with the scattering from pure PIB-H and pure PIB-d_8, the effect of multiple scattering being taken into account. The total (single and multiple) incoherent scattering per unit solid angle, $I_{H,i}$, from a pure PIB-H sample is given by

$$I_{H,i} = I_0 A[1 - \exp(-N_H \sigma_i t_H)]/4\pi \quad (1)$$

where I_0 is the incident beam intensity per unit area, A is the area of the sample, N_H the number of protons in PIB-H per unit volume, σ_i the incoherent scattering cross section of hydrogen, and t_H the thickness of the sample. Equation 1 was confirmed for PIB-H by measuring the scattering by pure PIB-H samples of three different thicknesses. Since eq 1 is valid for a system containing other coherent scatterers,[19] the incoherent background I_i from a sample containing protons can be evaluated in terms of $I_{H,i}$, from pure PIB-H, by use of the equation

$$I_i = \frac{1 - \exp(-N\sigma_i t)}{1 - \exp(-N_H \sigma_i t_H)} I_{H,i} \quad (2)$$

where N is the number of protons per unit volume of the sample and t is the thickness.

Inasmuch as the incoherent scattering cross section of deuterium is negligibly small compared with that of hydrogen, the scattering from PIB-d_8 can be considered almost entirely coherent in comparison with the scattering from PIB-H. Furthermore, the coherent scattering from both PIB-H and PIB-d_8 can be considered to be proportional to the coherent scattering cross sections, $\sigma_{H,coh}$ and $\sigma_{D,coh}$, of the monomer units of these polymers.[20] Therefore, the incoherent scattering from PIB-H can be calculated from the equation

$$I_{H,i} = I_H - \frac{t_H T_H \sigma_{H,coh}}{t_D T_D \sigma_{D,coh}} I_D \quad (3)$$

where I_H and I_D are the scattering from pure PIB-H and pure PIB-d_8 samples, respectively; T_H (T_D) and t_H (t_D) are the transmission and the thickness of the PIB-H (PIB-d_8) sample, respectively. We have assumed single scattering for coherent scattering. By combining eq 2 and 3, we can estimate the incoherent background due to protons in both PIB-H guest molecules and PIB-d_6 host molecules.

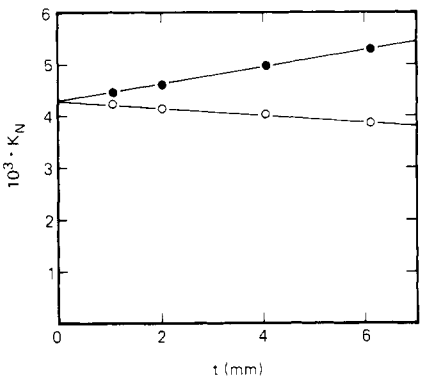

Figure 2. Determination of the parameter K_N for absolute intensity calibration using vanadium samples of various thicknesses t: (○) calculated from eq 5 and 6, taking into account multiple scattering; (●) calculated from eq 5 and 7 in the single scattering approximation.

(d) Coherent Background. The coherent background scattering due to the matrix was subtracted according to the theory of Akcasu et al.[21] by using the equation

$$I_{coh} = \left[1 + \left(\frac{a_{H,coh}}{a_{M,coh}} - 1\right)c\right]^2 I_{M,coh} \quad (4)$$

where I_{coh} is the coherent background to be subtracted, $a_{H,coh}$ and $a_{M,coh}$ are the scattering lengths of monomers of PIB-H and of the matrix polymer, respectively, c is the mole fraction of PIB-H monomers, and $I_{M,coh}$ is the coherent scattering from the pure matrix. For a fully deuterated PIB-d_8 matrix $I_{M,coh}$ may be replaced by I_D.

(e) Absolute Intensity Calibration. Absolute intensity calibrations were made with vanadium, water, a precalibrated irradiated aluminum sample, and a standard polystyrene dissolved in a Θ-solvent. After correction for multiple scattering effects, the observed differential cross section $(d\Sigma/d\Omega)$ per unit volume of a sample can be determined by the equation

$$\frac{d\Sigma}{d\Omega} = \frac{Ir^2}{I_0 \epsilon F A t T} \quad (5)$$

where t is the sample thickness, T the observed transmission, I the scattered intensity per detector element, and r the sample-to-detector distance; F and ϵ are the area and the average efficiency of the detector elements. Since the product ϵF remains constant for a fixed wavelength and electronic condition of the detector, the quantity $K_N \equiv I_0 \epsilon F$ can serve as the reference for absolute intensity calibration.[22]

The total scattering (single plus multiple) for a vanadium sample of thickness t can be approximated by the equation[23]

$$Ir^2/(I_0 \epsilon F A) = e^{-N\sigma_a t}(1 - e^{-N\sigma_i t})/4\pi \quad (6)$$

where N is the number of atoms per unit volume; σ_a and σ_i are the absorption and incoherent scattering cross sections of vanadium, respectively. The combination of eq 5 and 6 enables one to determine the value of K_N. On the other hand, the single scattering component may be approximated by[23]

$$d\Sigma/d\Omega = N\sigma_i/4\pi \quad (7)$$

An alternative value of K_N can be determined by combining eq 5 and 7.

Figure 2 shows the K_N values determined from measurements on vanadium samples of four different thicknesses. The values calculated by eq 5 and 6, shown by the open circles, decrease with increase of the sample thickness. This is because eq 6 does not take account of the increase of path lengths of the neutrons involved in multiple scattering, which are subject to more ab-

sorption than eq 6 allows. On the contrary, eq 7, in combination with eq 5, yields the K_N values shown by the filled circles that increase with sample thickness owing to neglect of multiple scattering. Both of these errors can be eliminated, as shown in Figure 2, by extrapolating the K_N values to infinitesimal thickness to obtain the correct value of K_N.

The incoherent scattering by water can also be used as a standard for the calibration. Disregarding the coherent scattering and absorption, one obtains for the total scattering

$$I/(I_0\epsilon FA) = (1 - e^{-N_H\sigma_i t})g/4\pi \quad (8)$$

The factor g takes into account of the contribution from the inelastic scattering, which is stronger in the forward direction. The value of g is approximated by $g^{-1} = 1 - \exp(-0.6\lambda^{1/2})$ according to Jacrot.[24] Combination of eq 5 and 8 enables one to determine the value of K_N. This method, however, always yielded slightly larger values than the other methods, probably because of underestimation of g.

A monodisperse polystyrene of molecular weight M = 100 000 dissolved in a Θ-solvent, cyclohexane-d_{12}, at 40 °C[25] also served as a standard sample for the absolute intensity calibration through use of the Zimm equation (cf. eq 12 below).

The K_N value was determined also by means of an irradiated aluminum sample, Al-5, calibrated with the Jülich FRJ2 SANS instrument by Hendricks, Schelten, and Schmatz[26] and made available to us at NCSASR.

All of the K_N values determined by the different methods described above agreed within an error or ±7% with the exception of the value obtained by using the water sample.

(4) X-ray Scattering. X-ray scattering was measured at the Stanford Synchrotron Radiation Laboratory with the radiation produced by the 4-GeV storage ring, SPEAR, at the Stanford Linear Accelerator Center. The radiation is monochromated by (220) reflections from two silicon crystals and collimated with a pair of pinholes located 25 cm apart. The wavelength of the monochromated X-rays was 1.65 Å ± 0.01%. The scattered intensity was measured with a one-dimensional position-sensitive proportional counter of 10 cm length and 1 cm width. The collimation error due to the finite width of the detector was minimized by attaching a sector-shaped mask in front of the detector window. The sample-to-detector distance was either 20 or 60 cm, and the size of the pinholes was 0.3 × 0.3 mm². A monitor counter consisting of a fluorescent screen and a photodiode was embedded in the beamstop, and the digital output from the monitor was accumulated every 2 s during the measuring time. Since the monitor counter measures the intensity of the incident beam after being attenuated by the sample, the monitor counts can be used to correct for the transmission of the sample as well as for the decay and fluctuation of the incident beam intensity. The inhomogeneity in detector sensitivity was corrected on the basis of measurements with isotopic radiation from ^{55}Fe. Absolute intensity calibrations were made by means of a standard polystyrene (M_w = 17 500) dissolved in cyclohexane at 35 °C, the Θ-temperature.[14]

Theoretical Scattering Functions

(1) Structure and Configuration. The structure of the PIB molecule is shown in Figure 1 of the preceding paper.[13] Configurational characteristics of PIB have been ascertained from the conformational energy calculations and the interpretation of them presented therein.[13] The skeletal bond angle at the methyl carbon is appreciably strained because of the severe steric repulsions by the two bulky methyl groups substituted at every second skeletal carbon atom. Four torsional angles are found[13] to provide an appropriate set of rotational isomeric states designated t_+, t_-, g_+^+, and g_-^-. These results are summarized in Table II, together with the bond lengths used in our calculations.

The statistical weight matrices for PIB chains are given by eq 15 and 16 of the preceding paper (I).[13] The conditional probability matrices required for the Monte Carlo calculations (cf. seq.) follow from eq 29 and 30 of I. With the parameter ζ assigned the value 0.0065,[13] appropriate for T = 300 K, they are

Table II
Parameters Used for Calculations of Scattering Functions

parameter	value
C–C bond length	1.53 Å[a]
C–H bond length	1.10 Å[a]
∠C^{s}C′C^s	123°
∠C′C^{s}C′	109°
torsion angle for t_+	15°
torsion angle for t_-	−15°
torsion angle for g_+^+	130°
torsion angle for g_-^-	−130°

[a] Values assigned according to crystallographic data.

$$Q' = \begin{array}{c} \\ t_+| \\ t_-| \\ g_+^+| \\ g_-^-| \end{array} \begin{array}{c} \begin{array}{cccc} |t_+ & |t_- & |g_+^+ & |g_-^- \end{array} \\ \begin{bmatrix} 0 & 0 & 0.9935 & 0.0065 \\ 0 & 0 & 0.0065 & 0.9935 \\ 0.9935 & 0.0065 & 0 & 0 \\ 0.0065 & 0.9935 & 0 & 0 \end{bmatrix} \end{array}$$

for the bond pair flanking the substituted skeletal carbon atom, and

$$Q'' = \begin{array}{c} \\ |t_+ \\ |t_- \\ |g_+^+ \\ |g_-^- \end{array} \begin{array}{c} \begin{array}{cccc} t_+| & t_-| & g_+^+| & g_-^-| \end{array} \\ \begin{bmatrix} 0.50 & 0 & 0.50 & 0 \\ 0 & 0.50 & 0 & 0.50 \\ 0.50 & 0 & 0.50 & 0 \\ 0 & 0.50 & 0 & 0.50 \end{bmatrix} \end{array}$$

for the bond pair within the diad bounded by successive substituted carbon atoms. The vertical bars in the row and column designations indicate locations of the substituted carbons of the chain skeleton. The a priori probability for each eligible rotational isomeric state is the same, i.e., p_ζ = 0.25 for all states ζ.

The positions of methyl carbons were considered to be fixed so that the plane defined by the bond pair CH_3–C^s–CH_3 is perpendicular to the plane defined by the bond pair CH_2–C^s–CH_2, where C^s denotes the substituted carbon in the same monomer unit. The bond angle CH_3–C^s–CH_3 was assumed to be the tetrahedral angle, i.e., 109.5°. The positions of methylene protons were fixed in a similar manner; the plane defined by the bond pair H–C′–H was treated as being perpendicular to the plane defined by the bond pair C^s–C′–C^s, where C′ denotes the methylene carbon, and the angle H–C′–H was assigned the value 109.5°. We adopted two different assumptions for the rotations of methyl groups: (a) they can rotate freely and noncooperatively, i.e., the rotation angles of all methyl groups are independent and can take any value between 0° and 360° with equal probability; and (b) they are fixed in the staggered position with respect to the other three bonds flanking the substituted carbon. The latter assumption is validated by the computations presented in I.[13]

(2) Scattering Functions. The scattering function $P(\mu)$ of a system of independent and randomly oriented molecules comprising N identical scattering elements is given by the equation

$$P(\mu) = \frac{1}{N^2}\left\langle \sum_i \sum_j \frac{\sin(\mu r_{ij})}{\mu r_{ij}} \right\rangle \quad (9)$$

where r_{ij} is the distance between the ith and jth scattering elements, and the angle brackets denote the statistical mechanical average over all configurations of the molecule. We assume that the scattering elements are small enough to be regarded as point scatterers, and we consider the

center of an atom to be the scattering locus for both neutron and X-ray scattering. The double sum in eq 9 can be reduced to a single sum by introducing the distance distribution function $h(r_k)$ or an angular average of the correlation function for the spatial distribution of the scattering elements. Adoption of the former alternative yields

$$P(\mu) = \frac{1}{N^2}\sum_k \langle h(r_k)\rangle \frac{\sin(\mu r_k)}{\mu r_k} \tag{10}$$

The function $h(r_k)$ represents the number of distances r_{ij} falling between $r_k - \Delta/2$ and $r_k + \Delta/2$, where Δ is an increment of r_k. The introduction of $h(r_k)$ can reduce the computing time consumed for repeated calculations of $\sin(\mu r_{ij})/\mu r_{ij}$. We adopted 0.01 Å as the value of Δ, which is well within the limits of precision of the structural data and conformational parameters.

Theoretical and experimental scattering data were compared by using Kratky plots with the Kratky function replaced by its analog of absolute magnitude defined by[11]

$$F_x(\mu) = (x + 1)\mu^2 P(\mu) \tag{11}$$

where $x + 1$ is the number of monomer units per chain.

Theoretical scattering functions were calculated by the Monte Carlo method, the positions of individual atoms being treated explicitly. Monte Carlo configurations were generated by assigning one of the four possible rotational isomeric states to successive bonds according to the applicable conditional probabilities. For a configuration thus generated, the positions of all scattering points were calculated by serial multiplication of the appropriate generator matrices for the chain vectors.[27] Then the distance between every pair of scattering points was calculated and stored in a linear array as the distance distribution function $h(r_k)$. This process was repeated for 100 Monte Carlo chains, each configuration being given an equal weight; the function $h(r_k)$ for each chain was accumulated, and the results were averaged over all chains.[28] A first approximation for the function $P(\mu)$ was calculated according to eq 10 from these data. Another 100 configurations were generated; the distance distributions were accumulated and combined with the previous array and reaveraged. A second approximation for $P(\mu)$ was then calculated on the basis of the function $h(r_k)$ averaged over 200 chains. This second approximation was compared with the preceding one, and the relative rms deviation was calculated. The procedure was repeated for an additional 100 chains, and so on. Iteration was continued until the rms deviation from the previous approximation fell below a preset value, taken to be 0.5%, the comparison being made in the range of $0 < \mu \leq 0.2$ Å^{-1} where the convergence is slowest. Usually 600 chains were sufficient to fulfill this criterion. The chains consisted of 900 monomer units. Scattering functions were calculated for the central 800 monomers, end effects thereby being eliminated. Thus, the calculated scattering functions are for chains of molecular weight 44 800, which is comparable to M_w of PIB-H used in the experiments (see Table I).

Scattering functions were calculated with the scattering points comprising (i) all eight protons of the PIB-H monomer, (ii) the six methyl protons, (iii) the two methylene protons, (iv) all four carbons, and (v) the substituted carbons only. The scattering function i is to be compared with the experimental data taken in the PIB-d_8 matrix and in the Θ-solvent, benzene-d_6. The function ii is appropriate for comparison with the scattering of PIH-H dispersed in PIB-d_6. The calculated scattering function iv is to be compared with the X-ray scattering data. The other two calculations are illustrative of the effects of differences in the scattering elements on the scattering functions.

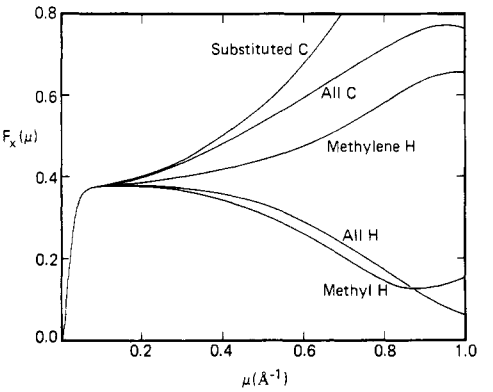

Figure 3. Theoretical absolute Kratky functions $F_x(\mu)$ for PIB computed with five different choices for scattering points as noted beside each curve and expressed in Å^{-2}. Calculations were carried out by the Monte Carlo procedure described in the text for chains composed of 800 monomer units embedded within chains of 900 monomers.

Figure 3 shows the results of these calculations. Despite the fact that all curves are derived from the same set of configurations, the differences among them are substantial at intermediate angles, i.e., for $\mu > 0.2$ Å^{-1}. These differences demonstrate the importance of accurately identifying the locations of the scattering elements. It can be seen that the scattering function at intermediate angles is dominated by the radius of gyration of the scattering elements in the cross section of the chain.

Assumptions (a) and (b) above concerning rotations of methyl groups yield nearly identical results, indicating that the methyl rotations have little effect on the shape of the scattering curve within the μ range shown in Figure 3. This result assures the reliability of these theoretical functions for our purposes and simultaneously indicates intermediate-angle scattering to be insensitive to very small distances on the order of a few angstrom units, as should be expected.

Results and Discussion

(1) Chain Dimensions. The weight-average molecular weight, M_w, and z-average radius of gyration, $\langle s^2\rangle_z^{1/2}$, of the protonated guest polymer dispersed in a deuterated matrix can be determined from the analysis in the Guinier region according to the Zimm equation

$$\frac{Kc(1-c)\rho}{(d\Sigma/d\Omega)^*} = \frac{1}{M_w}\left(1 + \frac{\langle s^2\rangle_z}{3}\mu^2\right) \tag{12}$$

with

$$K = N_A(a_H - a_D)^2/M_0^2 \tag{13}$$

where $(d\Sigma/d\Omega)^*$ is the excess coherent scattering cross section per unit volume of the sample, c and ρ are respectively the mole fraction (or volume fraction[29]) and density of the guest polymer, N_A is Avogadro's number, M_0 is the molecular weight of the guest monomer, and a_H and a_D are the scattering lengths of guest and host monomers, respectively. Equation 12 has been modified according to recent scattering theories[21,30,31] for a labeled polymer dispersed in the unlabeled counterpart of the same degree of polymerization; $c(1-c)\rho$ has been substituted for the polymer concentration in the original form. Where the degrees of polymerization and distributions of the host and guest molecules are not identical, $\langle s^2\rangle_z$ and $d\Sigma_{(0)}/d\Omega$ are replaced in eq 12 by apparent values that are functions of the numerical mismatch between the molec-

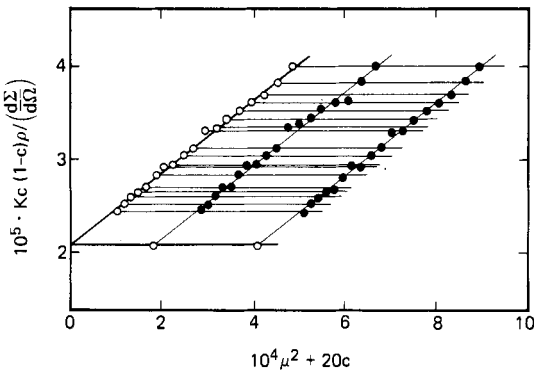

Figure 4. Zimm plot for neutron scattering by protonated PIB-H dispersed in the fully deuterated PIB-d_8 matrix. Measurements made at room temperature at volume fractions 0.1 and 0.2 of PIB-H.

Table III
Radii of Gyration and Molecular Weights of PIB-H Determined by Neutron Scattering

matrix or solvent	M_w	exptl $\langle s^2\rangle_z^{1/2}$, Å	exptl $\langle s^2\rangle_w^{1/2}$, Å	calcd $\langle s^2\rangle_w^{1/2}$, Å
PIB-d_8	48 000 ± 3000[a]	75 ± 5[a]	68 ± 5[b]	67–68[c]
benzene-d_6	52 000 ± 4000[a]	77 ± 5[a]	69 ± 5[b]	

[a] Determined from Figures 4 and 5. [b] Calculated from $\langle s^2\rangle_z^{1/2}$; see text. [c] Calculated from the averaged M_w = 48 700 and characteristic ratio C_∞ = 6.6–6.8.[13]

ular distributions. Small corrections for this effect were made by using methods developed by Boué, Nierlich, and Leibler.[32] For the analysis of dilute solutions in the Θ-solvent, we use the Zimm equation in its original form, in which a_D in eq 13 is naturally replaced by $(\bar{v}_H/\bar{v}_S)a_S$, where $\bar{v}_H$ and $\bar{v}_S$ are the partial specific volumes of the PIB-H monomer and of the solvent, respectively, and a_S is the scattering length of the solvent.

The completely flat scattering curve for pure PIB-d_8 confirmed the absence of void scattering, which often appears in experiments with a deuterated matrix, by virtue of the semiliquid character of the polymer.

Figures 4 and 5 show the Zimm plots for the neutron scattering by PIB-H dispersed in the PIB-d_8 matrix and dissolved in the Θ-solvent, respectively. Table III summarizes the results obtained from analysis of these plots. Values of $\langle s^2\rangle_z^{1/2}$ observed in the bulk and in the Θ-solvent are practically the same. This result confirms the theoretical prediction that the chain dimensions in these systems should be identical[10] and is in accord with other experimental observations.[33] Weight-average radii of gyration, $\langle s^2\rangle_w^{1/2}$, calculated from the observed $\langle s^2\rangle_z^{1/2}$ with correction for polydispersity according to[34]

$$\langle s^2\rangle_w = \langle s^2\rangle_z(1+u)/(1+2u)$$

where $u = M_w/M_n - 1$, are listed in Table III. They agree with the values estimated from the average molecular weight, M_w = 48 700, and the characteristic ratio, C_∞ = 6.6 – 6.8 (see Table I of I[13]), according to the relation $\langle s^2\rangle_w = (M_w/M_b)l^2C_\infty/6$, where M_b = 28 is the molecular weight per skeletal bond and l = 1.53 Å is the length of a skeletal bond. Although the molecular weights determined by neutron scattering are somewhat larger than the value from GPC/LS, they are still within the limit of the experimental uncertainty for the absolute intensity calibrations, i.e., ±7%. We may conclude therefore that the guest molecules are statistically distributed in the host matrix.[35]

(2) Chain Configurations. The absolute Kratky function $F_x(\mu)$ for the protonated PIB dispersed in a deuterated matrix can be evaluated in terms of experimentally observable variables by use of the equation

$$F_x(\mu) = \mu^2(d\Sigma/d\Omega)^*/Kc(1-c)\rho M_0 \qquad (14)$$

Figure 6 shows the $F_x(\mu)$ function plotted against μ for neutron scattering measurements on PIB-H dispersed in the fully-deuterated matrix, PIB-d_8. In order to cover the small-to-intermediate angular region up to μ = 0.6 Å^{-1}, measurements were made with four combinations of the sample-to-detector distance and wavelength, each run covering a consecutive range of μ as described in the legend to the figure. The long overlapped portions for consecutive runs and the smoothness in their connections confirm the accuracy of absolute intensity calibrations and other corrections. The measurements were performed at two different volume fractions of PIB-H, c = 0.1 and 0.2. No dependence on concentration is observed. The solid curve in Figure 6 shows the theoretical absolute Kratky function $F_x(\mu)$ calculated by the Monte Carlo method on the assumption that all eight protons in PIB-H monomers are scattering elements of equal scattering power. The agreement between the experimental and theoretical curves is excellent throughout the μ range of the measurements. The maximum value $\mu \simeq 0.6$ Å^{-1} at which the measurements were performed corresponds to distances of ca. 10 Å in real space, which is commensurate with segments of four monomers in all-trans conformations. We

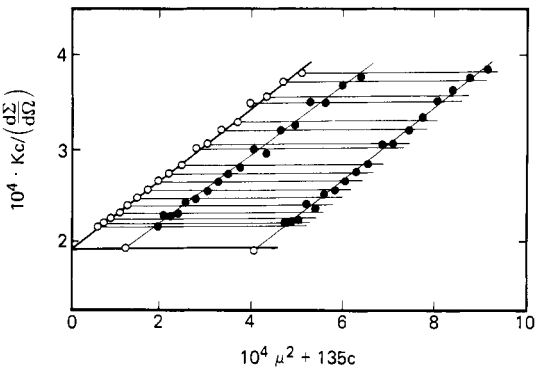

Figure 5. Zimm plot for neutron scattering by PIB-H dissolved in benzene-d_6 at 26.4 °C (Θ-temperature). Concentrations of PIB-H are 0.01 and 0.03 g/cm^3.

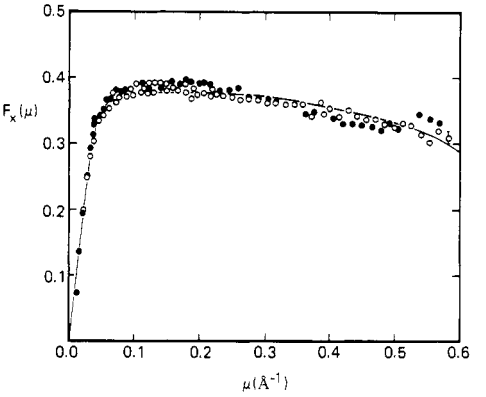

Figure 6. Absolute Kratky plots for neutron scattering by PIB-H dispersed in the fully deuterated PIB-d_8 matrix measured at volume fractions of 0.1 (●) and 0.2 (○). Measurements were carried out for four different combinations of wavelength λ and sample-to-detector distance L: λ = 4.75 Å and L = 12 m for $\mu \le 0.04$ Å^{-1}; λ = 4.75 Å and L = 4 m for 0.02 Å$^{-1} \le \mu \le 0.12$ Å^{-1}; λ = 2.38 Å and L = 4 m for 0.06 Å$^{-1} \le \mu \le 0.25$ Å^{-1}; λ = 2.38 Å and L = 1.3 m for 0.12 Å$^{-1} \le \mu \le 0.6$ Å^{-1}. The solid curve represents the theoretical function $F_x(\mu)$ calculated by the Monte Carlo method with scattering loci comprising all protons in PIB-H. The ordinate scale is in Å^{-2}.

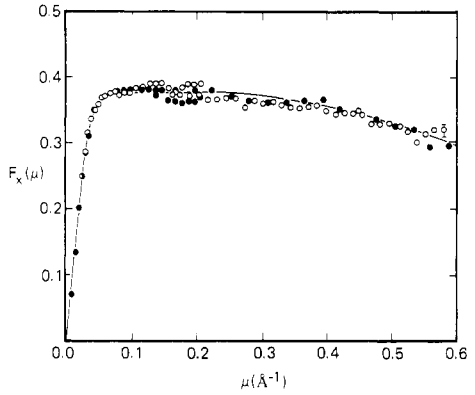

Figure 7. Absolute Kratky plots for neutron scattering by PIB-H dissolved in benzene-d_6 measured at 26.4 °C (Θ-temperature) at concentrations of 0.03 (●) and 0.06 g/cm^3 (○). Apparatus conditions and the theoretical curve shown by the solid line are the same as in Figure 6.

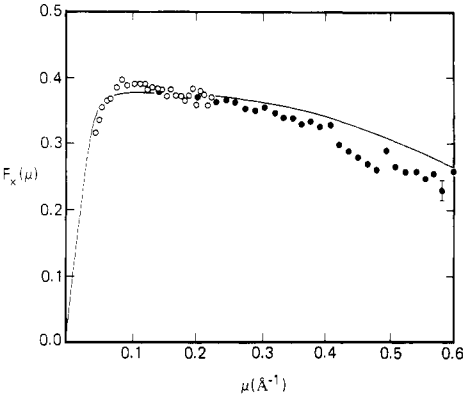

Figure 8. Absolute Kratky plots for neutron scattering by 0.27 volume fraction of PIB-H dispersed in the partially deuterated PIB-d_6 matrix. Measurements at two different sample-to-detector distances: L = 1.3 (●) and 4.0 m (○), with λ = 2.38 Å. The solid curve represents the theoretical function $F_x(\mu)$ calculated by the Monte Carlo method with scattering loci comprising methyl protons alone.

conclude, therefore, that the theoretical considerations based on the conformational energies and the rotational isomeric state scheme[13] precisely predict the configuration of PIB chains in the bulk down to segments comprising four monomers. It is also confirmed that the local configurations of individual chains in the bulk are random down to distances of ca. 10 Å in the sense that they are statistically unperturbed by intermolecular interactions such as might cause local ordering.

It is important to observe that the agreement between theory and experiment demonstrated in Figure 6 is achieved without aid of any adjustable parameters in the theoretical calculations. The calculations that follow are likewise fully determined by structural parameters and the conformational analysis.[13]

The absolute Kratky functions $F_x(\mu)$ for the neutron scattering by PIB-H dissolved in benzene-d_6 at 26.4 °C, the Θ-temperature, are shown in Figure 7. Measurements conducted under four different apparatus conditions, as in the experiments in bulk, are well represented by a single smooth curve. The measurements performed at two different polymer concentrations, 0.03 and 0.06 g/cm^3, give no evidence of concentration dependence. Absence of interchain interference in this concentration range is therefore indicated. The same theoretical curve shown in Figure 6 is represented by the solid line in Figure 7. Excellent agreement between the theoretical and experimental curves demonstrates that the theory predicts the chain configuration in the Θ-solvent with the same accuracy as in the bulk, likewise with 10-Å resolution.

Comparison of Figures 6 and 7 shows the experimental curves observed in the bulk and in the Θ-solvent to be indistinguishable throughout the μ range covered by the experiments. Since these scattering curves were measured on the same PIB-H molecules, it is scarcely conceivable that their concordance is merely a coincidence due to scattering equivalence. Therefore, we conclude that the configuration of PIB chains in the bulk and in the Θ-solvent are identical down to distances of ca. 10 Å or sequences of four monomer units. This result, together with the observation on radii of gyration, provides decisive proof that chain configurations in amorphous polymers are essentially unperturbed, as predicted from theoretical considerations.[10]

Figure 8 shows the $F_x(\mu)$ function for the neutron scattering by PIB-H observed in the partially-deuterated matrix, PIB-d_6. Since only methyl protons in PIB-H contribute to the excess coherent scattering in this experiment, interference among methyl groups is extracted

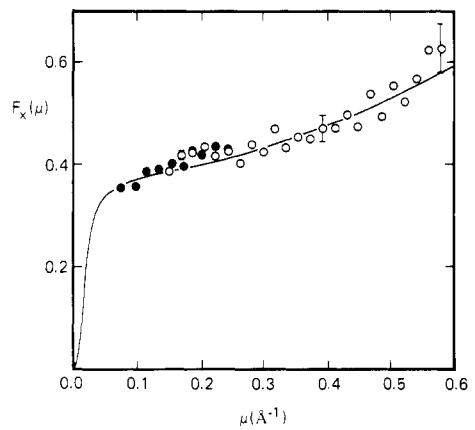

Figure 9. Absolute Kratky plot for X-ray scattering by PIB-H dissolved in n-heptane measured at 25.0 °C and at a concentration of 0.026 g/cm^3. Sample-to-detector distances L = 20 (○) and 60 cm (○), with λ = 1.65 Å. The solid curve shows the theoretical absolute Kratky function $F_x(\mu)$ calculated by the Monte Carlo method assuming all carbon atoms to be scattering points of equal scattering power.

by these data. The measurements were conducted at a volume fraction of 0.27 of PIB-H at two different sample-to-detector distances with a wavelength of 2.38 Å. Due to the abundant methylene protons in the matrix, the incoherent background scattering was relatively large, thus leading to a smaller signal-to-noise ratio than in the former cases, especially at larger μ values. The solid curve in Figure 8 represents the theoretical function $F_x(\mu)$ calculated for scattering points consisting of methyl protons alone. The experimental results and calculations are in good accord despite the higher background and the resulting larger range of error. They reconfirm the validity of the theoretical analysis and provide additional evidence for randomness of configurations in amorphous polymers. It is further to be noted that the marked difference between the degree of polymerization of PIB-d_6 compared with that of PIB-d_8 (see Table I) is without effect on the scattering by the guest, PIB-H.

Figure 9 shows the $F_x(\mu)$ function for X-ray scattering observed on PIB-H dissolved in n-heptane at 25 °C. The polymer concentration was 0.026 g/cm^3. Two different sample-to-detector distances were used to cover a wide range of μ. The solid curve represents the theoretical absolute Kratky function computed on the basis of the realistic model in which the centers of all carbon atoms

are taken as scattering loci. We prefer to assign an equal scattering power to each carbon rather than to add the scattering power of hydrogen to that of carbon. This assignment is justified by the following considerations. The excess electrons Z_e per scattering element in CH_3, CH_2, and C^s is given by

$$Z_e = Z - V\rho_1$$

where Z is the number of electrons per element, V is the volume of the element, and ρ_1 is the electron density of the solvent. If we take the van der Waals volume[36] as the volume of the element, the excess electrons are estimated as $Z_e(CH_3) = 3.6$, $Z_e(CH_2) = 4.0$, and $Z_e(C^s) = 4.7$, the difference in scattering power among the elements being ±13%. Therefore it is a reasonable simplification to attribute equal scattering power to each carbon center rather than to take the sum of the scattering powers of hydrogens and carbons.

We used *n*-heptane, a good solvent, in this experiment because of unavailability of an appropriate Θ-solvent for PIB-H yielding sufficient contrast in X-ray scattering. Therefore, we cannot discuss the comparison in the range of $\mu \leq 0.05$ Å^{-1}, where the excluded volume effect on the scattering function is appreciable. In the intermediate region, however, close agreement between the theoretical and experimental results was obtained, providing further evidence for the validity of the conformational analysis and the theoretical configurations deduced therefrom.

Acknowledgment. We are grateful to Prof. K. O. Hodgson and Dr. R. C. Miyake-Lye of Stanford University for assistance in the X-ray scattering measurements, to Prof. J. P. Kennedy of the University of Akron for preparation of the deuterated polymers, and to Dr. P. M. Cotts of IBM for measurements of GPC/LS. H.H. is indebted to Dr. D. Y. Yoon of the IBM Research Laboratory for helpful discussion and encouragement. H.H. acknowledges with gratitude a research fellowship provided by IBM Japan.

Registry No. Polyisobutylene, 9003-27-4; neutron, 12586-31-1.

References and Notes

(1) For instance, see reviews by: (a) Higgins, J.; Stein, R. S. *J. Appl. Crystallogr.* **1978**, *11*, 346 (b) Maconnachie, A.; Richards, R. W. *Polymer* **1978**, *19*, 739.
(2) Kirste, R. G.; Kruse, W. A.; Ibel, K. *Polymer* **1975**, *16*, 120.
(3) Kirste, R. G.; Kruse, W. A.; Schelten, J. *Makromol. Chem.* **1972**, *162*, 299.
(4) Cotton, J. P.; Decker, D.; Benoit, H.; Farnoux, B.; Higgins, J.; Jannink, G.; Ober, R.; Picot, C.; des Cloizeaux, J. *Macromolecules* **1974**, *7*, 863.
(5) Wignall, G. D.; Ballard, D. G. H.; Schelten, J. *Eur. Polym. J.* **1974**, *10*, 861.
(6) Schelten, J.; Ballard, D. G. H.; Wignall, G. D.; Longman, G.; Schmatz, W. *Polymer* **1976**, *17*, 751.
(7) Lieser, G.; Fischer, E. W.; Ibel, K. *J. Polym. Sci., Polym. Lett. Ed.* **1975**, *13*, 39.
(8) Ballard, D. G. H.; Cheshire, P.; Longman, G. W.; Schelten, J. *Polymer* **1978**, *19*, 397.
(9) Allen, G. A.; Tanaka, T. *Polymer* **1978**, 271.
(10) Flory, P. J. *J. Chem. Phys.* **1949**, *17*, 303; "Principles of Polymer Chemistry"; Cornell University Press: Ithaca, NY, 1953; *Macromol. Chem., Suppl. Pure Appl. Chem.* **1972**, *8*, 1.
(11) Fujiwara, Y.; Flory, P. J. *Macromolecules* **1970**, *3*, 288.
(12) Yoon, D. Y.; Flory, P. J. *Macromolecules* **1976**, *9*, 294, 299.
(13) Suter, U. W.; Saiz, E.; Flory, P. J. *Macromolecules*, preceding paper.
(14) Shultz, A. R.; Flory, P. J. *J. Am. Chem. Soc.* **1952**, *74*, 4760.
(15) Krigbaum, W. R.; Flory, P. J. *J. Am. Chem. Soc.* **1953**, *75*, 5254.
(16) Smelser, S. C.; Henninger, E. H.; Pings, C. J.; Wignall, G. D. *J. Appl. Crystallogr.* **1975**, *8*, 8.
(17) Koehler, W. C.; Hendricks, R. W. *J. Appl. Phys.* **1979**, *50*, 1951.
(18) Child, H. R.; Spooner, S. J. *J. Appl. Crystallogr.* **1980**, *13*, 259.
(19) The quantity in the angle brackets in eq 1 expresses the probability that incident neutrons are scattered incoherently at least once, irrespective of whether they are subject to coherent scattering at any other occasion.
(20) We assume that the structure factors of the monomers are angle-independent. This is justified because we are concerned with relatively small angles.
(21) Akcasu, A. Z.; Summerfield, G. C.; Jahshan, S. N.; Han, C. C.; Kim, C. Y.; Yu, H. *J. Polym. Sci., Polym. Phys. Ed.* **1980**, *18*, 863.
(22) Wignall, G. D. "User Notes for the 30 Meter SANS Instrument"; NCSASR, ORNL: Oak Ridge, TN, 1982.
(23) Wignall, G. D. UKAEA Research Group Memorandum 1928, H.M.S.O., London, 1967.
(24) Jacrot, B. *Rep. Prog. Phys.* **1976**, *39*, 911.
(25) Strazielle, G.; Benoit, H. *Macromolecules* **1975**, *8*, 203.
(26) Hendricks, R. W.; Schelten, J.; Schmatz, W. *Philos. Mag.* **1974**, *30*, 819.
(27) Flory, P. J. "Statistical Mechanics of Chain Molecules"; Wiley-Interscience: New York, 1969.
(28) In practice, this averaging, i.e., division by the number of chains, was done after $P(\mu)$ was computed using the accumulated function $h(r_k)$.
(29) We identify the mole fraction of monomers with the volume fraction in eq 12.
(30) Williams, C. E.; Nierlich, M.; Cotton, J. P.; Jannink, G.; Boué, F.; Daoud, M.; Farnoux, B.; Picot, C.; de Gennes, P.-G.; Rinaudo, M.; Moan, M.; Wolff, C. *J. Polym. Sci., Polym. Lett. Ed.* **1979**, *17*, 379.
(31) Wignall, G. D.; Hendricks, R. W.; Koehler, W. C.; Lin, J. S.; Wai, M. P.; Thomas, E. L.; Stein, R. S. *Polymer* **1981**, *22*, 886.
(32) Boué, F.; Nierlich, M.; Leibler, L. *Polymer* **1982**, *23*, 29.
(33) See Table II in ref 1a.
(34) Altgelt, K.; Schulz, G. V. *Makromol. Chem.* **1960**, *36*, 209.
(35) Schelten, J.; Wignall, G. D.; Ballard, D. G. H. *Polymer* **1974**, *15*, 682.
(36) Bondi, A. *J. Phys. Chem.* **1964**, *68*, 441.